Langmuir
Article
pubs.acs.org/Langmuir

Self-Assembled Monolayers of Double-Chain Disulfides of Adenine on Au: An IR-UV Sum-Frequency Generation Spectroscopic Study

Tetsuhiko Nagahara,[‡] Takumi Suemasu, Misako Aida, and Taka-aki Ishibashi*

Center for Quantum Life Sciences and Graduate School of Science, Hiroshima University, Kagamiyama, Higashi-Hiroshima, 739-8530, Japan. [‡]*Present address: Department of Chemistry and Materials Technology, Kyoto Institute of Technology, Matsugasaki, Kyoto 606-8585, Japan.*

Received June 18, 2009. Revised Manuscript Received September 2, 2009

We have synthesized double-chain disulfides of adenine with different chain lengths ($n = 2$, 4, 5, 9, and 10) and studied their self-assembled monolayers (SAM) on gold surface by IR-UV doubly resonant sum frequency generation spectroscopy with the help of DFT calculation. A versatile way to investigate the orientation angle of functional groups of SAMs and their surface coverage has been demonstrated. It was revealed that the IR dipoles of the band at around 1630 cm^{-1}, which were almost parallel to the long molecular axis of the adenine ring, were less tilted with respect to the substrate surface in the SAMs with longer chains ($n = 9$ and 10) in comparison to those with shorter chains ($n = 2$, 4, and 5).

Introduction

Molecular recognition and hydrogen bond formation between nucleic acid bases have been extensively studied in connection to Watson−Crick base pairing in DNA or to molecular recognition, for example, enzymes and cofactors. Interactions between bases on the surface of self-assembled monolayers (SAMs) and complementary bases in a solution or gas phase were also studied in this regard.[1−4] The attractive interactions between complementary bases are applicable to chemical force microscopy or adhesion map AFM, which may enable the reading of sequences of a DNA directly in the near future by forming a SAM of a base on an AFM tip.[5]

On the basis of these viewpoints, SAMs of adenine derivatives on gold substrates have been studied. It is known that optimal surface density of adenine is crucial for the specific binding of uracil, which is an analogue of complementary Watson−Crick counterpart of thymine, to adenine since adenine−adenine homointeractions and interactions between adenine and hydrophobic groups in the SAM may hinder the adsorption of uracil.[3,4] It is also known that there exists some non-Watson−Crick binding modes (e.g., Hoogsteen binding mode), in which different sets of hydrogen-bonding sites function and which may alter the binding specificities of the bases. That is to say, the binding sites of the SAM should be directed to the binding species. Thus, it is important to estimate orientations of the hydrogen-bonding sites or the adenine ring in the SAMs. The purpose of this study is to demonstrate the effectiveness of IR-UV doubly resonant sum-frequency generation (DR-SFG) spectroscopy as a tool to investigate the orientation angle of aromatic functional groups, especially DNA bases, in SAMs. We synthesized double-chain disulfides of adenine (A) derivatives of various alkyl chain lengths [compounds **3**, $A-(CH_2)_n-S-S-(CH_2)_n-A$; $n = 2$, 4, 5, 9 and 10] and examined their SAMs on gold surfaces.

Orientations and conformations of SAM forming molecules can be studied by surface specific vibrational spectroscopies which probe vibrational resonances of functional groups in the molecule on the surface, such as reflection absorption IR spectroscopy (RAIRS) and vibrationally resonant sum-frequency generation spectroscopy (SFG), since these spectroscopies utilize polarized light.[6−9] We attempted to examine SAMs of alkylated adenines by RAIRS at first, but the spectra obtained were poor in quality for determination of molecular orientation because of a high and sloping background that could not be subtracted in the fingerprint region.

In contrast, we obtained vibrational spectra of the SAMs, which were in high quality and were affected little by the background, by DR-SFG spectroscopy which utilizes both IR and UV polarized lasers and which enabled us to probe the bases in SAMs selectively with high sensitivity rather than to probe the whole SAM forming molecules because of the electronic resonant effect.[10−13] We investigated the orientation of adenine moieties at the top of the SAMs of different lengths of alkyl chains by analyzing the DR-SFG spectra with the help of vibrational analyses using quantum chemical calculations.

Experimental Section

General. Water was purified to a resistivity of ∼18 MΩ cm by a water purification system (Arium 611UV, Sartorius). All organic solvents and reagents were used without further purification unless otherwise noted. ^1H NMR spectra of dimethylsulfoxide (DMSO) d^6 or $CDCl_3$ solutions were recorded on a JEOL

*To whom correspondence should be addressed Fax: +81-82-424-0727. E-mail: taib@hiroshima-u.ac.jp.

(1) Kurihara, K.; Ohto, K.; Honda, Y.; Kunitake, T. *J. Am. Chem. Soc.* **1991**, *113*, 5077–5079.
(2) Calvo, E. J.; Rothacher, M. S.; Bonazzola, C.; Wheeldon, I. R.; Salvarezza, R. C.; Vela, M. E.; Benitez, G. *Langmuir* **2005**, *21*, 7907–7911.
(3) Matsuura, K.; Ebara, Y.; Okahata, Y. *Langmuir* **1997**, *13*, 814–820.
(4) Weisser, M.; Käshammer, J.; Menges, B.; Matsumoto, J.; Nakamura, F.; Ijiro, K.; Shimomura, M.; Mittler, S. *J. Am. Chem. Soc.* **2000**, *122*, 87–95.
(5) Sunami, H.; Ijiro, K.; Karthaus, O.; Kraemer, S.; Mittler, S.; Knoll, W.; Shimomura, M. *Mol. Cryst. Liq. Cryst.* **2001**, *371*, 151–154.
(6) Allara, D. L.; Nuzzo, R. G. *Langmuir* **1985**, *1*, 52–66.
(7) Ihs, A.; Uvdal, K.; Liedberg, B. *Langmuir* **1993**, *9*, 733–739.
(8) Wang, J.; Chen, C.; Buck, S. M.; Chen, Z. *J. Phys. Chem. B* **2001**, *105*, 12118–12125.
(9) Zhuang, X.; Miranda, P. B.; Kim, D.; Shen, Y. R. *Phys. Rev. B* **1999**, *59*, 12632–12640.
(10) Raschke, M. B.; Hayashi, M.; Lin, S. H.; Shen, Y. R. *Chem. Phys. Lett.* **2002**, *359*, 367–372.
(11) Ishibashi, T.; Onishi, H. *Appl. Phys. Lett.* **2002**, *81*, 1338–1340.
(12) Ishibashi, T.; Onishi, H. *Appl. Spectrosc.* **2002**, *56*, 1298–1302.
(13) Maeda, T.; Ishibashi, T. *Appl. Spectrosc.* **2007**, *61*, 459–464.

Scheme 1. Synthesis of Double-Chain Adenine Disulfides [A−$(CH_2)_n$−S−S−$(CH_2)_n$−A; n = 2, 4, 5, 9, and 10]

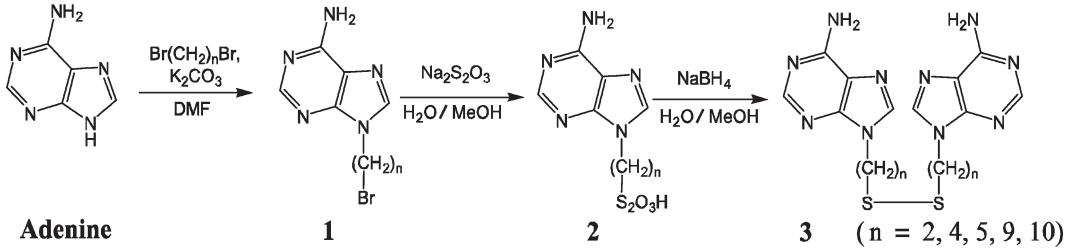

GSX500 (500 MHz) spectrometer. Chemical shifts were reported in parts per million relative to tetramethylsilane. IR spectra of adenine disulfides were observed as KBr pellets or solutions of DMSO on a Nicolet 6700 FT-IR spectrometer (Thermoelectron) equipped with an LN-cooled MCT detector. Reflection absorption IR spectra (RAIRS) of the adenine SAMs on gold substrates were recorded with the FT-IR spectrometer equipped with a reflectance accessory (Specac). The incident angle of the *P*-polarized probe beam was set at 80 degrees from the surface normal. Raman spectra of the adenine disulfides were observed as powder on a Raman spectrometer (NRI-1866M, JASCO) equipped with an Ar^+ ion laser (514.5 nm, Spectra Physics). UV absorption spectra of adenine disulfide solutions in a 1-mm cuvette were recorded by an absorption spectrometer (V-570, JASCO). Vibrational analyses using quantum chemical calculations of model molecules were carried out by the B3LYP method with the basis set 6-31G* using the Gaussian 03 program package.[14] The harmonic wavenumbers, the IR transition dipoles, and the preresonance Raman tensors excited at 260 nm were calculated on an energy-optimized geometry of the molecule. The harmonic wavenumbers were scaled by the wavenumber-linear scaling (WLS) method.[15]

SFG Apparatus. The details of our SFG spectrometer using wavelength-tunable optical parametric amplifiers (OPAs) and multiplex detection scheme can be found elsewhere.[11−13] Briefly, our light sources were based on an amplified Ti:Sapphire laser (2.5 mJ, 1 kHz, TITAN-II, Quantronix). Femtosecond broadband IR probe pulses (∼2 μJ at ∼1600 cm^{-1}, ∼200 cm^{-1} fwhm) and picosecond narrow-band UV pulses (∼0.1 μJ, ∼8 cm^{-1} fwhm) were generated by using femtosecond and picosecond OPAs (TOPAS, Light Conversion), respectively. It should be noted that an SFG spectrometer that is both IR and UV wavelength tunable is indispensable to satisfy the doubly resonant condition of the adenine moiety. The two input probe pulses were overlapped spatially and temporally on the sample, and the sum-frequency (SF) signal generated was analyzed with a spectrograph [asymmetric double spectrograph consisting of a prism premonochromator stage (CT-25UV, JASCO) and a grating polychromator stage (TRIAX550, Horiba Jobin Yvon)]/LN-cooled CCD (Roper Scientific) combination. A GaAs(110) wafer was used as a reference of the SFG signal. The polarization directions of SF, UV, and IR beams were *P*, *P*, and *P*, respectively. The incidence angles of UV and IR beams were 70 and 50 degrees relative to the surface normal, respectively.

Cyclic Voltammetry. Reductive desorption of SAMs on the substrates, which were mounted at a hole of an electrochemical cell by an elastic O-ring, were measured using a potentiostat (Hokuto Denko). The surface area of the electrode was calculated to be 0.5 cm^2 from the diameter of the O-ring. A basic solution of aqueous KOH (0.5 M) in the cell was degassed with Ar for 15 min prior to the measurements. The potential (E) is referred to an Ag|AgCl electrode. Scan rate was set to a value of 50 mV s^{-1}.

Materials. Double-chain adenine disulfides were synthesized by alkylation of adenine followed by subsequent introduction of thiosulfate to form disulfides (see below) as shown in Scheme 1. SAMs of the alkylated adenines were formed on gold-on-mica substrates (Picosubstrate, Molecular Imaging) by immersing the substrates in ∼1 mM ethanol solutions of the disulfides (compounds **3**) for about 12 h unless otherwise stated. It is known that molecules having disulfide groups form chemisorbed SAMs on gold as thiolates efficiently.[16,17] To minimize contamination, the gold substrates were cleaned by soaking in a chromic acid solution (Wako Pure Chemical), which strongly oxidizes organic contaminants, for about 12 h prior to use and then rinsed with ultrapure water and ethanol. Immediately after the cleaning, they were immersed into the ethanol solutions of adenine disulfides for deposition. After removal from the solution, the substrate was rinsed thoroughly with copious ethanol to remove physisorbed molecules and was brown dried with nitrogen gas.

Synthesis of Compounds 1. Alkylhalides of adenine [compounds **1**, A−$(CH_2)_n$−Br; n = 2, 4, 5, 9, and 10] were synthesized as described in the literature.[18,19] Adenine (10 mmol) was alkylated with α,ω-dibromoalkanes (45 mmol) in DMF (75 mL) in the presence of potassium carbonate (30 mmol) under nitrogen atmosphere. The solutions were stirred at room temperature for 24−48 h. Compounds **1** were extracted with chloroform and washed with saturated NaCl aq. After evaporation of the solvent, the products [A−$(CH_2)_n$−Br; n = 2, 4, 5, 9, and10] were purified by a preparative silica gel column (eluted by ethyl acetate−methanol mixture = 85:15) and by crystallization from methanol.

n = 2:. 82% yield; ^{1}H NMR (500 MHz, DMSO d^6, δ ppm) 8.17 (1H, s, C*H*), 8.14 (1H, s, C*H*), 7.25 (2H, s, NH_2), 4.57 (2H, t, CH_2), 3.95 (2H, t, CH_2).

n = 4:. 41% yield; ^{1}H NMR (500 MHz, DMSO d^6, δ ppm) 8.15 (1H, s, C*H*), 8.14 (1H, s, C*H*), 7.20 (2H, s, NH_2), 4.18 (2H, t, CH_2), 3.55 (2H, t, CH_2), 1.93 (2H, q, CH_2), 1.75 (2H, q, CH_2).

n = 5:. 72% yield; ^{1}H NMR (500 MHz, DMSO d^6, δ ppm) 8.15 (1H, s, C*H*), 8.12 (1H, s, C*H*), 7.18 (2H, s, NH_2), 4.14 (2H, t, CH_2), 3.51 (2H, t, CH_2), 1.82 (4H, m, CH_2), 1.35 (2H, q, CH_2).

(14) Frisch, M. J.; Trucks, G. W.; Schlegel, H. B.; Scuseria, G. E.; Robb, M. A.; Cheeseman, J. R.; Montgomery, J.A. J.; Vreven, T.; Kudin, K. N.; Burant, J. C.; Millam, J. M.; Iyengar, S. S.; Tomasi, J.; Barone, V.; Mennucci, B.; Cossi, M.; Scalmani, G.; Rega, N.; Petersson, G. A.; Nakatsuji, H.; Hada, M.; Ehara, M.; Toyota, K.; Fukuda, R.; Hasegawa, J.; Ishida, M.; Nakajima, T.; Honda, Y.; Kitao, O.; Nakai, H.; Klene, M.; Li, X.; Knox, J. E.; Hratchian, H. P.; Cross, J. B.; Bakken, V.; Adamo, C.; Jaramillo, J.; Gomperts, R.; Stratmann, R. E.; Yazyev, O.; Austin, A. J.; Cammi, R.; Pomelli, C.; Ochterski, J. W.; Ayala, P. Y.; Morokuma, K.; Voth, G. A.; Salvador, P.; Dannenberg, J. J.; Zakrzewski, V. G.; Dapprich, S.; Daniels, A. D.; Strain, M. C.; Farkas, O.; Malick, D. K.; Rabuck, A. D.; Raghavachari, K.; Foresman, J. B.; Ortiz, J. V.; Cui, Q.; Baboul, A. G.; Clifford, S.; Cioslowski, J.; Stefanov, B. B.; Liu, G.; Liashenko, A.; Piskorz, P.; Komaromi, I.; Martin, R. L.; Fox, D. J.; Keith, T.; Al-Laham, M. A.; Peng, C. Y.; Nanayakkara, A.; Challacombe, M.; Gill, P. M. W.; Johnson, B.; Chen, W.; Wong, M. W.; Gonzalez, C.; Pople, J. A., *Gaussian 03*, revision D.01; Gaussian: Wallingford, CT, **2004**.

(15) Yoshida, H.; Takeda, K.; Okamura, J.; Ehara, A.; Matsuura, H. *J. Phys. Chem. A* **2002**, *106*, 3580–3586.

(16) Taniguchi, I.; Toyosawa, K.; Yamaguchi, H.; Yasukouchi, K. *J. Chem. Soc., Chem. Commun.* **1982**, *18*, 1032–1033.

(17) Nuzzo, R. G.; Allara, D. L. *J. Am. Chem. Soc.* **1983**, *105*, 4481–4483.

(18) Fkyerat, A.; Demeunynck, M.; Constant, J.-F.; Michon, P.; Lhomme, J. *J. Am. Chem. Soc.* **1993**, *115*, 9952–9959.

(19) Itahara, T. *J. Chem. Soc., Perkin. Trans.* **1998**, *2*, 1455–1462.

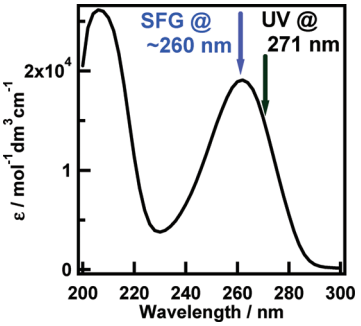

Figure 1. UV absorption spectrum of a representative double-chain disulfide of adenine ($n = 2$) in ethanol (7.8×10^{-5} M). The spectra of unsubstituted adenine and other adenine derivatives with different chain lengths (not shown) were almost identical in this spectral region.

n = 9:. 67% yield; ^{1}H NMR (500 MHz, $CDCl_3$, δ ppm) 8.37 (1H, s, C*H*), 7.80 (1H, s, C*H*), 5.59 (2H, s, NH_2), 4.19 (2H, t, CH_2), 3.40 (2H, t, CH_2), 1.91−1.26 (14H, m, CH_2).

n = 10:. 73% yield; ^{1}H NMR (500 MHz, $CDCl_3$, δ ppm) 8.38 (1H, s, C*H*), 7.79 (1H, s, C*H*), 5.59 (2H, s, NH_2), 4.19 (2H, t, CH_2), 3.40 (2H, t, CH_2), 1.91−1.26 (16H, m, CH_2).

Synthesis of Compounds 2. Thiosulfate compounds [compounds **2**, A−$(CH_2)_n$−S_2O_3H; n = 2, 4, 5, 9, and 10] were synthesized as described in the literature.[20,21] Compounds **1** (4 mmol) and sodium thiosulfate pentahydrate (4 mmol) in 35 mL solvent (water for n = 2, 4 and 5; water−methanol mixture = 1:1 for n = 9 and 10) were refluxed for 2.5 h. After completion of the reaction, aqueous hydrochloric acid was added to the reaction mixtures at room temperature, and the mixtures were cooled on ice to obtain solid products. The solid products (compounds **2**) were washed thoroughly with ice-cold water and dried in vacuo.

n = 2:. 95% yield; ^{1}H NMR (500 MHz, DMSO d^6, δ ppm) 8.46 (1H, s, C*H*), 8.43 (1H, s, C*H*), 4.60 (2H, t, CH_2), 3.29 (2H, t, CH_2).

n = 4:. 81% yield; ^{1}H NMR (500 MHz, DMSO d^6, δ ppm) 8.51 (1H, s, C*H*), 8.43 (1H, s, C*H*), 4.25 (2H, t, CH_2), 2.86 (2H, t, CH_2), 1.92 (2H, q, CH_2), 1.64 (2H, q, CH_2).

n = 5:. 91% yield; ^{1}H NMR (500 MHz, DMSO d^6, δ ppm) 8.52 (1H, s, C*H*), 8.45 (1H, s, C*H*), 4.24 (2H, t, CH_2), 2.51 (2H, t, CH_2), 1.83 (2H, q, CH_2), 1.68 (2H, q, CH_2), 1.30 (2H, q, CH_2).

n = 9:. 65% yield; ^{1}H NMR (500 MHz, DMSO d^6, δ ppm) 8.48 (1H, s, C*H*), 8.43 (1H, s, C*H*), 4.23 (2H, t, CH_2), 2.66 (2H, t, CH_2), 1.81 (2H, q, CH_2), 1.58 (2H, q, CH_2), 1.33−1.20 (10H, m, CH_2).

n = 10:. 57% yield; ^{1}H NMR (500 MHz, DMSO d^6, δ ppm) 8.51 (1H, s, C*H*), 8.45 (1H, s, C*H*), 4.22 (2H, t, CH_2), 2.65 (2H, t, CH_2), 1.81 (2H, q, CH_2), 1.58 (2H, q, CH_2), 1.33−1.20 (12H, m, CH_2).

Synthesis of Compounds 3. Disulfide compounds [compounds **3**, A−$(CH_2)_n$−S−S−$(CH_2)_n$−A; n = 2, 4, 5, 9, and 10] were synthesized as described in the literature.[21] Aqueous sodium borohydride (10%) was poured into solutions of compounds **2** (0.7 mmol) in 5 mL solvent (water for n = 2, 4 and 5; water−methanol mixture = 1:1 for n = 9 and 10), and the mixtures were stirred for 6 h. The products (compounds **3**) were filtered, washed thoroughly with ice-cold water and purified by crystallization from chloroform.

n = 2:. 90% yield; ^{1}H NMR (500 MHz, DMSO d^6, δ ppm) 8.13 (1H, s, C*H*), 8.13 (1H, s, C*H*), 7.21 (2H, s, NH_2), 4.42 (2H, t, CH_2), 3.25 (2H, t, CH_2).

n = 4:. 78% yield; ^{1}H NMR (500 MHz, DMSO d^6, δ ppm) 8.14 (1H, s, C*H*), 8.13 (1H, s, C*H*), 7.19 (2H, s, NH_2), 4.16 (2H, t, CH_2), 2.65 (2H, t, CH_2), 1.86 (4H, q, CH_2), 1.53 (4H, q, CH_2).

(20) Distler, H. *Angew. Chem., Int. Ed. Engl.* **1967**, *6*, 544–553.
(21) Tsalmane, L. V.; Lidak, M. J. *Bioorg. Khim.* **1990**, *16*, 976–980.

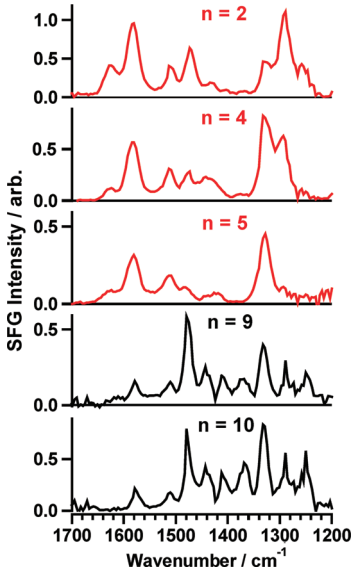

Figure 2. DR-SFG spectra of double-chain adenine disulfides [A−$(CH_2)_n$−S−S−$(CH_2)_n$−A; n = 2, 4, 5, 9 and 10] SAMs on gold substrates.

Table 1. Band Positions (in cm^{-1}) and Band Intensities (Normalized by the Reference Signal, Shown in Parentheses) Obtained for Double-Chain Disulfides of Adenine [A−$(CH_2)_n$−S−S−$(CH_2)_n$−A] SAMs on Gold from SFG Experiments

n = 2	n = 4	n = 5	n = 9	n = 10
1629 (0.017)	1636 (0.024)	1637 (0.020)		
1581 (0.085)	1582 (0.11)	1580 (0.029)	1577 (0.0051)	1578 (0.010)
1511 (0.013)	1512 (0.026)	1509 (0.014)	1504 (0.0048)	1513 (0.0049)
1472 (0.049)	1477 (0.010)	1481 (0.022)	1477 (0.050)	1479 (0.018)
1430 (0.029)	1436 (0.062)	1435 (0.0067)	1441 (0.025)	1433 (0.065)
1405 (0.0014)	1432 (0.061)	1420 (0.0069)	1413 (0.039)	1413 (0.046)
1374 (0.00088)	1374 (0.0011)		1366 (0.0085)	1363 (0.026)
1332 (0.016)	1333 (0.062)	1330 (0.067)	1334 (0.027)	1332 (0.063)
1291 (0.068)	1289 (0.044)	1301 (0.0019)	1290 (0.0091)	1293 (0.016)
1249 (0.019)	1250 (0.0035)		1247 (0.0066)	1249 (0.016)

n = 5:. 71% yield; ^{1}H NMR (500 MHz, DMSO d^6, δ ppm) 8.13 (2H, s, C*H*), 8.13 (2H, s, C*H*), 7.14 (4H, s, NH_2), 4.13 (4H, t, CH_2), 2.63 (4H, t, CH_2), 1.81 (4H, q, CH_2), 1.59 (4H, q, CH_2).

n = 9:. 51% yield; ^{1}H NMR (500 MHz, $CDCl_3$, δ ppm) 8.37 (2H, s, C*H*), 7.79 (2H, s, C*H*), 5.74 (4H, s, NH_2), 4.19 (4H, t, CH_2), 2.66 (4H, t, CH_2), 1.91−1.26 (30H, m, CH_2).

n = 10:. 58% yield; ^{1}H NMR (500 MHz, $CDCl_3$, δ ppm) 8.37 (2H, s, C*H*), 7.79 (2H, s, C*H*), 5.79 (4H, s, NH_2), 4.19 (4H, t, CH_2), 2.66 (4H, t, CH_2), 1.91−1.26 (32H, m, CH_2).

Results and Discussion

UV absorption spectrum of double-chain disulfide of adenine (compounds **3**, n = 2) in ethanol was measured as shown in Figure 1. The spectrum maximized at 261 nm and was almost identical to that of unsubstituted adenine. In the following part of the SFG experiments, we fixed the UV probe wavelength at 271 nm to satisfy an electronic resonant condition of adenine moiety at a sum-frequency wavelength (~260 nm).

As mentioned before, the orientations of functional groups of molecules in SAMs can be studied, in principle, by RAIRS. We attempted to do this, but instead, we obtained spectra by RAIRS with poor quality in the fingerprint region for determination of adenine orientation because of a high and sloping background that could not be precisely subtracted.

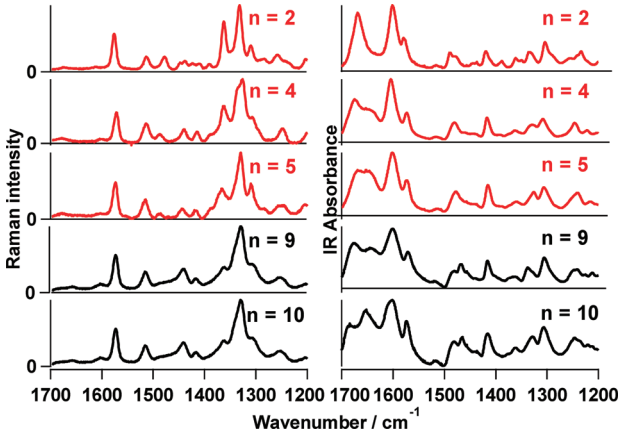

Figure 3. Raman and IR spectra of polycrystalline form of double-chain adenine disulfides. Polycrystalline powder and those in KBr were used in Raman and IR experiments, respectively.

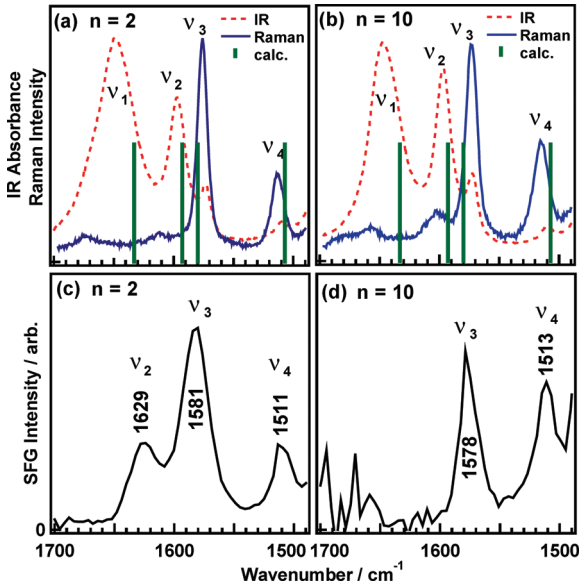

Figure 4. (a and b) IR (in DMSO, dashed curves) and Raman (polycrystalline, solid curves) spectra of randomly oriented samples (n = 2 and 10) and the DFT calculated wavenumbers (straight lines). The solvent bands are subtracted in the IR spectra. (c and d) For comparison, SFG spectra of SAM (the same as that shown in Figure 2) are also shown. The fine structures in panel d above 1650 cm^{-1} are because of the experimental error.

SFG spectra of adenine SAMs of different chain lengths (n=2, 4, 5, 9 and 10) obtained in the 1700−1200 cm^{-1} region are shown in Figure 2. The spectra were acquired several times in a day to confirm that they are reproducible. The band positions and intensities obtained are summarized in Table 1. The spectral features of SAMs with shorter chains (n = 2, 4, 5) in the 1650−1350 cm^{-1} region are quite different from those with longer chains (n = 9, 10): Intensities are of comparable order for ~1630 and ~1510 cm^{-1} bands for SAMs with shorter chains, while the intensities at ~1630 cm^{-1} are negligibly small compared to those at ~1510 cm^{-1} for SAMs with longer chains. It is known that vibrational bands resulting from the NH_2 scissoring and ring vibrations of adenine appear in the 1650−1500 cm^{-1} region.[22] The orientations of adenine in n=(2, 4, 5) and n=(9, 10) SAMs may be thus quite different if the bands observed by SFG were ascribed to

(22) Kyogoku, Y.; Lord, R. C.; Rich, A. *J. Am. Chem. Soc.* **1967**, *89*, 496–504.

Table 2. Harmonic Wavenumbers Obtained by DFT Calculations for Alkylated Adenines[a]

	9-methyladenine	9-ethyladenine	9-decyladenine
ν_1	1633	1633	1632
ν_2	1596	1593	1593
ν_3	1582	1580	1580
ν_4	1515	1507	1507
ν_5	1494	1482	1483
ν_6	1479	1481	1481
ν_7	1441	1470	1467
ν_8	1419	1422	1422
ν_9	1378	1388	1388
ν_{10}	1336	1360	1360
ν_{11}	1343	1340	1340
ν_{12}	1320	1319	1320
ν_{13}	1239	1285	1270
ν_{14}	1262	1256	1259
ν_{15}			1255
ν_{16}			1244
ν_{17}		1226	1220
ν_{18}	1203	1203	1204

[a] Vibrational modes ascribed to almost pure vibrations of alkyl chains are omitted in this table. The wavenumbers are scaled by the WLS method.[15]

that of adenine. On the other hand, spectral features in the 1350−1200 cm^{-1} region change gradually with increasing chain length up to n=5 and then change drastically to complex ones in n=9 and 10. The change of the spectra in the 1350−1200 cm^{-1} region may be due to change of vibrational modes caused by different alkyl-chain length and/or by the orientational change of adenine moieties.

To gain insight into the assignments of the observed SFG vibrational bands, we measured and compared vibrational spectra (IR and Raman) of orientationally averaged (isotropic) samples, polycrystalline solids, and DMSO solutions of adenine disulfides of different chain lengths. The spectra of polycrystalline samples are shown in Figure 3. Since SFG can be considered as IR excitation followed by anti-Stokes Raman transition, one has to consider both IR and Raman spectra. The IR spectra of a sample in KBr and in solution (not shown) were similar.

In contrast to the SFG spectra of the SAMs, all the IR spectra and also Raman spectra, are quite similar in the 1650−1500 cm^{-1} region, regardless of the chain length. This evidence suggests that the differences observed by the SFG experiments in the 1650−1500 cm^{-1} region are because of the orientation changes of adenine moiety in the SAMs.

It is not surprising that the IR spectral feature above 1650 cm^{-1} is absent in the SFG spectra shown in Figure 2, since the feature is known to be ascribed to almost pure NH_2 vibration, which is less likely to be enhanced by the electronic resonant effect of adenine ring in the DR SFG. In addition, it is known that NH_2 deformation modes, which may be observed in the 1700−1650 cm^{-1} region, are sensitive to the surrounding environments.[22,23] The surrounding environments, in this case, are alkyl chains or adenine rings of adjacent molecules and the solvent molecules in polycrystalline solids and in DMSO solutions, respectively. The wavenumbers of the NH_2 deformation mode in solutions and in polycrystalline solids were thus slightly different, as shown in Figures 4a and b.

Spectral features in IR and Raman below 1500 cm^{-1} change substantially with chain length, similar to that shown in the SFG spectra. This suggests that the SFG spectral changes below

(23) Wiorkiewicz-Kuczera, J.; Karplus, M. *J. Am. Chem. Soc.* **1990**, *112*, 5324–5340.

Table 3. Wavenumbers Obtained by Experiments and Calculations for Representative Adenine Derivatives (n = 2 and 10) in the 1650−1500 cm^{-1} region[a]

	DFT calculation		IR (solution)		Raman (powder)		DR SFG (SAM)		Assignments
	(n = 2)	(n = 10)	(n = 2)	(n = 10)	(n = 2)	(n = 10)	(n = 2)	(n = 10)	(DFT calc.)
ν_1	1633	1632	1649	1648	1674	1659			NH_2
ν_2	1593	1593	1597	1597	1609	1603	1629		ring, NH_2
ν_3	1580	1580	1573	1573	1576	1573	1581	1578	ring, NH_2
ν_4	1507	1507	1510	1510	1513	1515	1511	1513	ring, NH_2, CH_2

[a] Assignments based on the DFT calculation are also shown. The wavenumbers obtained by DFT calculations are scaled by the WLS method.[15]

1500 cm^{-1} are not necessarily caused by orientation effects, but by changes in vibrational modes because of different chain lengths, and hence vibrational modes of alkyl chain may be involved in the vibrational bands below the 1500 cm^{-1} region. In the following part of this paper, we will focus on the 1650−1500 cm^{-1} region that is expected to provide direct information on the orientation of the adenine group.

Vibrational analyses were conducted with the help of density-functional theory (DFT) calculation. The harmonic wavenumbers obtained for 9-methyl, 9-ethyl, and 9-decyladenine, which are scaled by the WLS method, are shown in Table 2. Vibrational modes assigned to almost pure vibrations of alkyl chains are omitted from the table. The agreement of the calculated wavenumbers between 9-ethyl and 9-decyladenine is better than that between 9-methyl and 9-ethlyadenine, except for the modes below 1300 cm^{-1}, which are quite complex and may be coupled to the alkyl chains. This finding suggests that the ethyl group is long enough to predict the influence of the alkyl chain to adenine vibrations, especially for those with wavenumbers larger than 1500 cm^{-1}. In the following part of this paper, we use 9-ethyladenine as the model molecule.

In Figure 4 and Table 3, spectra and wavenumbers of representative adenine disulfides with shorter and longer chains, n = 2 and 10, respectively, are compared with the calculated wavenumbers. The assignments of the modes are also shown in Table 3. It is clear that the ∼1510 cm^{-1} bands observed are assigned to ν_4 (1507 cm^{-1}) and the ∼1580 cm^{-1} bands to ν_3 (1580 cm^{-1}), respectively, since the wavenumbers obtained by experiments and calculation coincide very well. The IR spectra of KBr pellets (Figure 3, right panel) change with increasing chain length, while the spectra of DMSO solutions (Figures 4a and b) are very similar irrespective of the chain length. The change observed in KBr may be the result of interactions with surrounding alkyl chains.

The bands in IR/Raman spectra (1648−1674 cm^{-1}), which are absent in the SFG spectra, are assigned to the calculated ν_1 mode (1633 cm^{-1}), since ν_1 is assigned to almost pure vibration of NH_2 which may not resonate electronically in SFG experiments. The difference between the observed and the calculated wavenumbers of the ν_1 mode can be explained by the different environments around the NH_2 groups as described before. Regarding the different environments around the NH_2 groups, Kyogoku et al. reported that the scissoring mode of hydrogen bonded 9-ethyladenine was located at 1642 cm^{-1}, while that of the free form was at 1629 cm^{-1}.[22]

We assigned the remaining bands observed at 1629 cm^{-1} by SFG and observed at 1597−1609 cm^{-1} by IR/Raman to ν_2. The discrepancies between the observed (in powder and SAMs) and the calculated wavenumbers (in a vacuum) of the ν_2 mode, in which NH_2 vibration may be involved in part (see assignments in Table 2), can also be explained by the different environments around the NH_2 groups. The observed shifts of ν_2 band between the polycrystalline and solution samples (Figure 4a and b) support these findings.

From Figures 2 and 4, it is clear that the vibrational bands of ν_2, ν_3 and ν_4 are observed in SAMs of shorter chain lengths (n = 2, 4 and 5) while the bands of ν_3 and ν_4 are observed in SAMs of longer chain lengths (n = 9 and 10) by DR-SFG experiments. It should be noted here that all the three vibrational bands (ν_2, ν_3, and ν_4) were observed in the spectra of isotropic samples (solution and polycrystalline solid), and the spectra were very similar in their features regardless of the chain length. Consequently, the differences in the observed SFG spectral patterns in the 1650−1500 cm^{-1} region are not caused by the change in the vibrational modes, but to the change in the orientation of the adenine ring.

To elucidate the orientations of adenine ring in the SAMs from the observed DR SFG spectra, we used IR transition dipoles and Raman tensors of 9-ethyladenine calculated by DFT. The SFG signal intensity (I) is described as follows:

$$I \propto |\chi^{(2)}_{PPP}|^2 \tag{1}$$

The effective nonlinear susceptibility of $\chi^{(2)}_{PPP}$ for the PPP polarization combination in azimuthally isotropic case is described as follows:[8,9]

$$\begin{aligned}\chi^{(2)}_{PPP} = {} & -L_{XX}(\omega_{SF})L_{XX}(\omega_{UV})L_{ZZ}(\omega_{IR})\cos\theta_{SF}\cos\theta_{UV}\sin\theta_{IR}\chi^{(2)}_{XXZ} \\ & -L_{XX}(\omega_{SF})L_{ZZ}(\omega_{UV})L_{XX}(\omega_{IR})\cos\theta_{SF}\sin\theta_{UV}\cos\theta_{IR}\chi^{(2)}_{XZX} \\ & +L_{ZZ}(\omega_{SF})L_{XX}(\omega_{UV})L_{XX}(\omega_{IR})\sin\theta_{SF}\cos\theta_{UV}\cos\theta_{IR}\chi^{(2)}_{ZXX} \\ & +L_{ZZ}(\omega_{SF})L_{ZZ}(\omega_{UV})L_{ZZ}(\omega_{IR})\sin\theta_{SF}\sin\theta_{UV}\sin\theta_{IR}\chi^{(2)}_{ZZZ}\end{aligned} \tag{2}$$

where the ω and θ values are the respective frequencies and beam angles from the surface normal, and the L values are Fresnel factors related to the refractive indices and the angles; a laboratory Cartesian coordinate system (X, Y, Z) is chosen so that Z is along the surface normal and X is in the plane of incidence. $L_{XX}(\omega_{IR})$ and $L_{YY}(\omega_{IR})$ were evaluated to be negligibly small compared to $L_{ZZ}(\omega_{IR})$ because the substrate is gold. Thus we calculated the first and forth term in eq 2[8,9] in our experimental conditions by using the refractive index of gold.[24] As a result, we obtained

$$\chi^{(2)}_{PPP} = -0.266\chi^{(2)}_{XXXZ} + 1.256\chi^{(2)}_{ZZZ} \tag{3}$$

The nonlinear susceptibility, $\chi^{(2)}_{ijk}$, of the laboratory coordinates is related to a second-order molecular hyperpolarizability tensor of a molecular frame (l, m, n), $\beta^{(2)}_{lmn}$, as follows:

$$\chi^{(2)}_{ijk} \propto N \sum_{l,m,n} \langle(\hat{i}\cdot\hat{l})(\hat{j}\cdot\hat{m})(\hat{k}\cdot\hat{n})\rangle \beta_{lmn}{}^{(2)} \tag{4}$$

(24) Lynch, D. W.; Hunter, W. R. In *Handbook of Optical Constants of Solids*; Palik, E. D., Eds.; Academic. Press.: San Diego, CA, 1985; pp 286−295.

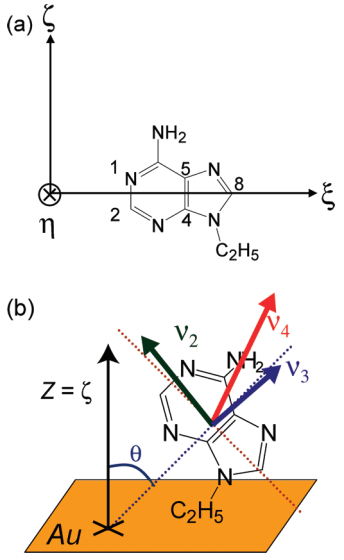

Figure 5. Molecular model used to analyze the orientations of adenine ring from the observed SFG spectra. (a) The standard orientation of the adenine moiety and molecular Cartesian coordinate system (ξ, η, ζ) are chosen. (b) The adenine group is rotated by tilt angle (θ) around η axis. The tilt angle (θ) of adenine from the surface normal, $Z = \zeta$, is defined as shown in the figure. Arrows indicate IR transition dipoles of the ν_2, ν_3, and ν_4 modes. Note that the IR transition moments of ν_3 and ν_4 are almost perpendicular to that of ν_2.

where N is the surface density of the molecules, and the angular bracket denotes an average over the molecular orientations. The hyperpolarizability is described as follows:

$$\beta^{(2)}_{lmn} = A_{lm}\mu_n \tag{5}$$

where A_{lm} and μ_n denote anti-Stokes Raman tensor and infrared transition dipole, respectively. From eq 5, SFG can be considered as an infrared excitation of a vibrational mode followed by an anti-Stokes Raman transition. Therefore, the electronic resonance effects of DR-SFG at sum-frequency wavelengths arise from the Raman tensor.

We choose the standard orientation of the adenine moiety and molecular Cartesian coordinate system (ξ, η, ζ) as shown in Figure 5a, such that ξ is along the line from the center of positions 1 and 2 to position 8 in the adenine ring, and the $\xi\zeta$ plane is parallel to the adenine ring. The calculated IR transition dipoles (μ) and the Raman tensors (A) of ν_2, ν_3, and ν_4 modes at the standard orientation are represented in the molecular Cartesian coordinate system as follows:

$$\begin{aligned}
\nu_2: &\begin{bmatrix} -10.0 \\ -0.55 \\ 1.34 \end{bmatrix}, \begin{bmatrix} 51.4 & 0.44 & -23.9 \\ 0.58 & -0.15 & -0.04 \\ -23.3 & -0.15 & 9.26 \end{bmatrix} \\
\nu_3: &\begin{bmatrix} -0.04 \\ 1.59 \\ 6.05 \end{bmatrix}, \begin{bmatrix} 14.5 & 0.05 & 0.10 \\ 0.05 & -0.07 & -0.31 \\ 0.10 & -0.31 & -7.94 \end{bmatrix} \\
\nu_4: &\begin{bmatrix} -0.42 \\ 0.32 \\ 4.32 \end{bmatrix}, \begin{bmatrix} -49.1 & -0.50 & 32.9 \\ -0.69 & 0.14 & 0.48 \\ 33.4 & 0.69 & -23.1 \end{bmatrix}
\end{aligned} \tag{6}$$

When the adenine group is rotated by θ around η, the resultant IR dipoles (μ') and Raman tensors (A') are obtained by using

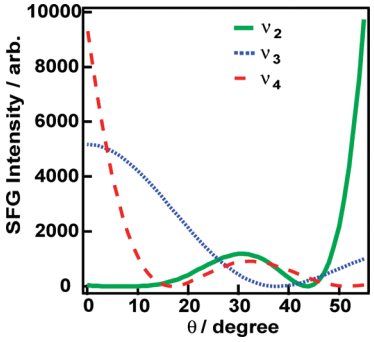

Figure 6. Calculated SFG intensities of the ν_2, ν_3, and ν_4 modes against tilt angle, θ. Solid (green), dotted (blue), and dashed curves (red), respectively, indicate calculated SFG intensities of the ν_2, ν_3, and ν_4 modes against the tilt angle θ.

rotation matrix T as follows:

$$\begin{aligned} \mu' &= T\mu \\ A' &= TA'T \end{aligned}; T = \begin{bmatrix} \cos\theta & 0 & \sin\theta \\ 0 & 1 & 0 \\ -\sin\theta & 0 & \cos\theta \end{bmatrix} \tag{7}$$

By assuming the adenine plane to be perpendicular to the substrate surface (see below) and random orientation about $Z = \zeta$ axis (azimuthally isotropic), the nonlinear susceptibilities shown on the right-hand side of eq 3 are described as follows:

$$\begin{aligned} \chi^{(2)}_{ZZZ} &\propto A'_{\zeta\zeta}\mu'_{\zeta} \\ \chi^{(2)}_{XXZ} &\propto \frac{A'_{\xi\xi} + A'_{\eta\eta}}{2}\mu'_{\zeta} \end{aligned} \tag{8}$$

The schematic illustration of the molecular orientation model used in this paper is shown in Figure 5b. The rotation angle of the adenine ring around the C4−C5 axis is fixed in the model. By using eqs 1 and 3−8 and assuming δ-function distribution of θ, SFG intensities of the ν_2, ν_3, and ν_4 modes are simulated against θ in a similar manner described in the literature (Figure 6).[8,9,25]

By comparing the SFG intensity ratios of the ν_2 and ν_3 modes, $I_{\nu 2}/I_{\nu 3}$ (and also $I_{\nu 4}/I_{\nu 3}$ for the ν_4 and ν_3 modes), obtained from the experiment (Table 1) and from the simulation (Figure 6), tilt angles of 20−30 or 40−45 degrees for n = (2, 4, 5) and 0−10 degrees for n = (9, 10), samples are deduced. Although we cannot uniquely specify the tilt angle for n = (2, 4, 5) samples, we can obtain valuable information from them. It has thus been concluded that the tilt angle of adenine with longer chains [0−10 degrees for n = (9, 10)] are less than those with shorter chains [20−30 or 40−45 for n = (2, 4, 5)]. It should be noted that the IR dipole of the ν_2 mode is located almost parallel to the substrate surface at a tilt angle of 0−10 degrees.

SFG intensities are in proportion to a square of the surface coverage (N^2), as well as to the component of $|\beta^{(2)}|^2$ as shown in eqs 1 and 4. Therefore, once the orientation angles of adenine ring are determined, their relative molecular area densities can be deduced based on the orientation angles and relative SFG intensities (of a certain mode) of different SAMs.

Ideal SFG intensities per molecule in an arbitrary unit, which is deduced from the DFT calculations and the model (see previous), were calculated for the obtained tilt angles (θ). The ratios of the ideal intensities of 0−10 and 20−30 degrees were 3.4×10^{-5}−0.1, 2.0−12, and 1.2−74, while those of 0−10 and 40−45 degrees were

(25) Hirose, C.; Akamatsu, N.; Domen, K. *Appl. Spectrosc.* **1992**, *46*, 1051–1072.

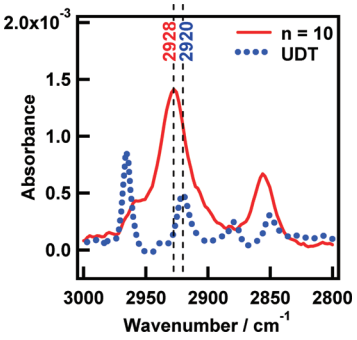

Figure 7. RAIRS spectra of an adenine SAM (n = 10, solid curve) and an undecanethiol (UDT, dotted curve) SAM on gold. Peak position of CH_2 antisymmetric stretching band of the adenine SAM (2928 cm^{-1}) is higher than that of the UDT SAM (2920 cm^{-1}).

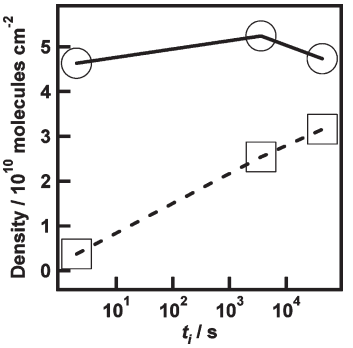

Figure 8. Surface coverage of SAMs at different immersion times (t_i = 2 s, 1 h, and 12 h) determined by the desorption peaks in the cyclic voltammograms. Open circles with solid lines and open squares with dashed lines indicate the surface densities of short-chain (n = 2) and long-chain (n = 10) SAMs of adenine at the specified times, respectively. The surface density of the long-chain SAM increases with increasing t_i, while that of the short-chain SAM remains constant.

1.8×10^{-5}−0.67, 2.0−12, and 4.7−560 for the ν_2, ν_3, and ν_4 modes, respectively. By comparing these values with the experimentally obtained SFG intensity ratios calculated from Table 1, relative molecular area densities of the SAMs with different chain lengths were estimated. The estimation is based on the fact that the quotient of the experimental band intensity ratio to the ideal intensity ratio is proportional to the squares of the surface coverage of the SAMs. The estimated surface coverages of the SAMs revealed that the densities of the SAMs with longer chains [n = (9, 10)] were less than 60% of those with shorter chains [n = (2, 4, 5)].

In general, long-chain alkane thiols form densely packed crystalline-like structures with extended alkyl chains tilted at an angle of 20−30 degrees.[26] This tilt angle of the all-trans alkyl chain corresponds to 0−10 degrees for the tilt angle of adenine (θ) in our model, which apparently agrees with that obtained for our long-chain SAMs. We compared RAIRS spectrum of adenine SAM with that of undecanethiol (UDT) in the CH_2 stretching region (Figure 7). The peak position of CH_2 antisymmetric vibration of the adenine SAM (n = 10) was located at 2928 cm^{-1}, while that of UDT SAM was at 2920 cm^{-1}. The peak position of the short-chain (n = 5) adenine SAM was located at 2927 cm^{-1} (not shown), while that of hexanethiol was reported to be at 2921 cm^{-1}.[26] It is known that peak position of the antisymmetric CH_2 vibration in the liquid phase is higher than that in the crystalline phase;[26] therefore, our observations suggest that the alkyl chains of the n = 10 and n = 5 SAMs are more likely to be in an unorganized liquid-like state than in a crystalline phase. In this connection, Weisser et al. also reported an unorganized SAM consisting of adenine thiol.[4] Although our observations suggest that alkyl chains of the long-chain and short-chain adenine SAMs form liquid-like rather than crystalline-like structure of unsubstituted alkane thiol SAMs,[26] the difference of the peak positions between the unsubstituted and the adenine SAMs are smaller in the short-chain SAMs suggesting more dense structures for the short-chain SAMs. This is qualitatively consistent with the results on the relative surface coverage obtained from the SFG spectra.

One might expect that steric hindrance between the bulky adenine moieties may be involved in the unorganized liquid-like alkyl chain in the adenine SAM. However, our results on relative surface coverage are in considerable contrast to that reported for the bulky cyclodextrin SAMs with different chain lengths, where higher density structures were suggested for the long-chain SAM with respect to the short-chain SAM.[27,28] Some interactions other than the steric hindrance, for example, π−π interaction between adenines and/or chain−chain interaction, may also be involved in our adenine SAMs.

It was reported that the SAM forming process, in general, comprises two steps: The initial step of diffusion controlled adsorption is followed by the second process of crystallization of alkyl chains.[29] We speculate that the chemisorption process during SAM formation is highly disturbed by the disordered alkyl chain in long-chain adenine disulfides compared to that in short-chain ones, and the disordered structures cannot be crystallized to form a densely packed crystalline-like molecular assembly at the surface in the second step due to the bulky terminal group, in contrast to the unsubstituted alkane thiolates.

The mechanism we described above was confirmed by comparing the SFG spectra of different immersion times (t_i), 1 and 12 h. The spectra of short-chain SAMs (n = 2) of different t_is were identical, while all the band intensities increased by a factor of ~1.5 with increasing t_i in the spectra of long-chain SAMs (n = 10). It was found that the molecular orientations were not affected by the immersion times in this time regime, since the spectral shapes of SAMs of respective chain lengths were very similar and independent of the immersion times. From eqs 1 and 4, the increase in band intensities corresponds to an increase of ~22% of the surface density in the duration for the long-chain SAM. Thus the SAM formation process in the long-chain SAMs should be highly disturbed and slower compared to the short-chain SAMs.

To make sure that the relative density estimation from the SFG results are correct, we measured electrochemical desorption of SAMs of different t_is (2 s, 1 h, and 12 h) by using cyclic voltammetry, which can quantify the thiolates.[30] The reductive desorption of the SAMs of the disulfides were observed at approximately E = −0.9 and −1.0 V for n = 2 and 10 SAMs, respectively. The molecular densities of SAMs were calculated from the area under the peaks in the cyclic voltammograms and the surface area of the electrodes by assuming completely flat Au surface (Figure 8). Regardless of immersion times, the surface densities of short-chain SAMs are very similar even at t_i = 2 s. The

(26) Porter, M. D.; Bright, T. B.; Allara, D. L.; Chidsey, C. E. D. *J. Am. Chem. Soc.* **1987**, *109*, 3359–3568.

(27) Weisser, M.; Nelles, G.; Wohlfart, P.; Wenz, G.; Mittler-Neher, S. *J. Phys. Chem.* **1996**, *100*, 17893–17900.
(28) Qian, J.; Hentschke, R.; Knoll, W. *Langmuir* **1997**, *13*, 7092–7098.
(29) Ulman, A. *Chem. Rev.* **1996**, *96*, 1533–1554.
(30) Walczak, M. M.; Popenoe, D. D.; Deinhammer, R. S.; Lamp, B. D.; Chung, C.; Porter, M. D. *Langmuir* **1991**, *7*, 2687–2693.

density of long-chain SAM, however, increases with increasing t_i; a density increase of 24% was observed in the 1−12 h regime. The relative densities of the short-chain and the long-chain SAMs obtained by SFG are thus consistent with those obtained by the quantitative electrochemical measurements.

We have thus far discussed the tilt angles and the densities of the adenine ring on the assumption that the plane of the adenine ring is perpendicular to the substrate surface, where the rotation angle around the C4−C5 axis (i.e., short molecular axis of the adenine ring) is fixed. If this is not the case and the adenine group is rotated substantially out of the $\zeta\xi$ plane around the C4−C5 axis, a significant decrease in the SFG intensity of ν_2 mode would be expected compared to those of ν_3 and ν_4 modes. This is because the rotation decreases the Z-component of the IR transition dipole for the ν_2 mode, while it does not for ν_3 and ν_4 whose dipoles are almost parallel to the C4−C5 axis. Therefore the assumption may be valid, especially for the short chain SAMs where the SFG signal of ν_2 mode was observed.

For the long-chain SAMs, however, the SFG signals of the ν_2 modes were not observed, and the assumption is thus not necessarily valid. It should be noted that there is another possible model for the orientation of the adenine group, which can explain the SFG spectra of the long-chain SAMs. In this alternative model, the adenine ring is rotated around the C4−C5 axis to decrease the μ_z so that the SFG signal of the ν_2 mode almost disappears irrespective of the tilt angle (θ). Again the IR dipole of the ν_2 mode may be located almost parallel to the substrate surface in long-chain SAMs. Thus it should be clear that the dipoles of the ν_2 mode of the long-chain SAMs are less tilted with respect to the substrate surface than those of the short-chain SAMs, regardless of the rotation angle around the C4−C5 axis. The surface densities of adenine in SAMs, however, can not be obtained from the observed SFG intensities by the latter model incorporating both the rotation and the tilt.

In conclusion, we have synthesized and studied orientation angles of adenine ring on SAMs with different alkyl chain lengths by IR-UV DR-SFG with the help of DFT calculation. Although the orientation angles of the base obtained may be different if the adenine SAMs are diluted by other SAM forming molecules (e.g., alkanethiol without adenine moiety such as UDT), since a decrease in adenine−adenine interactions and an increase in chain−chain interactions are expected, we are sure that our method provides a versatile way to study the orientation angles of the base. In future work, we would like to extend this study to the base pairs on SAMs.

Acknowledgment. The authors thank Prof. Keiichi Ohno and Dr. Yukiteru Katsumoto of Hiroshima University for FT-IR measurements, and NBARD of Hiroshima University for NMR and Raman spectrum measurements. The authors also thank Prof. Kohji Maeda of Kyoto Institute of Technology for electrochemical measurements. This work was supported in part by Grant-in-Aids for Scientific Research from the Ministry of Education, Culture, Sports, Science and Technology (MEXT) of the Japanese Government [No. 19056007, Priority Areas (477)] and NaBiT program.

Supporting Information Available. Cyclic voltammograms of short-chain (n = 2) and long-chain (n = 10) adenine SAMs on gold-on-mica substrates at different immersion times (t_i). This material is available free of charge via the Internet at http://pubs.acs.org.

Note Added after ASAP Publication. This article was published ASAP on September 22, 2009. Because of a production error, equation 7 was rendered incorrectly. The correct version was published on September 30, 2009.